https://doi.org/10.5194/bg-2020-175
Preprint. Discussion started: 2 July 2020

Biogeosciences Discussions
Open Access
EGU

Contrasting responses of woody and herbaceous vegetation to altered rainfall characteristics in the Sahel

Wim Verbruggen[1,2], Guy Schurgers[2], Stéphanie Horion[2], Jonas Ardö[3], Paulo Negri Bernardino[4,5], Bernard Cappelaere[6], Jérôme Demarty[6], Rasmus Fensholt[2], Laurent Kergoat[7], Thomas Sibret[1], Torbern Tagesson[2,3], and Hans Verbeeck[1]

[1]CAVElab, Department of Environment, Ghent University, Ghent, 9000, Belgium
[2]Department of Geosciences and Natural Resource Management, University of Copenhagen, Copenhagen, 1350, Denmark
[3]Department of Physical Geography and Ecosystem Science, Lund University, Lund, 22100, Sweden
[4]Department of Earth and Environmental Sciences, KULeuven, Leuven, 3000, Belgium
[5]Laboratory of Geo-Information Science and Remote Sensing, Wageningen University, Wageningen, 6708, The Netherlands
[6]HydroSciences Montpellier, IRD/CNRS, Université de Montpellier, Montpellier, 34090, France
[7]Géosciences Environnement Toulouse, CNRS/UPS/IRD, Toulouse, 31400, France

Correspondence to: Wim Verbruggen (wim.verbruggen@ugent.be)

https://doi.org/10.5194/bg-2020-175
Preprint. Discussion started: 2 July 2020

Biogeosciences Discussions

Abstract. Dryland ecosystems form a major land cover, accounting for about 40% of Earth's terrestrial surface and net primary productivity, and housing more than 30% of the human population. These ecosystems are subject to climate extremes (e.g. large-scale droughts) that are projected to increase in frequency and severity under most future climate scenarios. In this modelling study we assessed the impact of single years of extreme (high or low) rainfall on dryland vegetation in the Sahel. The magnitude and legacy of these impacts were quantified on both the plant functional type and the ecosystem levels. In order to understand the signature of the rainy season characteristics, these rainfall anomalies were driven by changing either rainfall intensity, event frequency or season length. The Lund-Potsdam-Jena General Ecosystem Simulator (LPJ-GUESS) dynamic vegetation model was parameterized to represent dryland plant functional types (PFTs) and was validated against fluxtower measurements across the Sahel. Different scenarios of extreme rainfall were derived from existing Sahel rainfall products such that meteorological consistency was maintained, and applied during a single year of the model simulation timeline. Herbaceous vegetation responded immediately to the different scenarios, while woody vegetation had a weaker and slower response, integrating precipitation changes over a longer timeframe. An increased season length had a larger impact than increased intensity or frequency, while impacts of decreased rainfall scenarios were strong and independent of the season characteristics. Soil control on surface water balance explains these contrasts between the scenarios. Semi-arid ecosystems are known to play a dominant role in the trend and variability of the terrestrial CO2 sink. We showed that single extremely dry and wet years can have strong and long-term impact on the productivity of drylands ecosystems, shedding new light on potential drivers and mechanisms behind this variability.

1 Introduction

Dryland ecosystems account for about 40% of Earth's terrestrial surface and net primary productivity (Grace et al., 2006; Wang et al., 2012), and shelter more than 30% of the human population (Gilbert, 2011). These ecosystems are subject to climate extremes that are projected to increase in frequency and severity under most future climate scenarios (IPCC, 2014; Sillmann et al., 2013). Such extremes (e.g., large extent droughts) can have a devastating impact on the ecosystems and livelihoods of global drylands, as well as amplifying pressure on fragile economic structures (Ibrahim, 1988; United Nations Office for the Coordination of Humanitarian Affairs, 2013). The Sahel, situated south of the Sahara desert, is one of the largest dryland areas of the world, covering more than 3 million km^2. It is home to a population of around 135 million people, which is expected to increase by a factor of 2.3 between 2014 and 2050 (Haub and Toshiko, 2014).

The Sahel is mostly dominated by savanna grasslands. These complex biomes consist of a sparse cover of C_3 trees and shrubs, overlying an understory dominated by C_4 grasses. The co-existence of herbaceous and woody species in drylands has been the subject of many studies (e.g., Dodd et al., 1998; McMurtrie and Wolf, 1983; van Wijk and Rodriguez-Iturbe, 2002), and can be explained by different strategies in root-water access and phenology. Disturbances such as wildfires can have a major impact on the tree cover as well, especially in mesic regions (mean annual precipitation (MAP) > 650 mm) (Sankaran et al., 2008). Capturing these complex ecosystems with dynamic vegetation models can be challenging, yet rewarding

https://doi.org/10.5194/bg-2020-175
Preprint. Discussion started: 2 July 2020

(Whitley et al., 2017) as these models can provide novel insights in the dynamics of tree-grass competition for resources, as well as dryland ecosystem carbon and water cycling in general.

Although the vegetation structure and ecosystem productivity in water-limited ecosystems is mainly driven by annual total precipitation (Lehmann et al., 2014; Sankaran et al., 2005, 2008), intra-annual rainfall variability, which is characterized by the variability in rain event intensity, frequency and timing of the wet season, has a large impact on the vegetation as well, by changing the spatial and temporal availability of soil water for plant uptake (Berry and Kulmatiski, 2017; Case and Staver, 2018; Guan et al., 2018; Kulmatiski and Beard, 2013; Xu et al., 2018; Zhang et al., 2018, 2019). The year-to-year variation in these characteristics is significant in the Sahel (Zhang et al., 2017). Climate projections for the end of the 21st century generally show a delay in timing of the rainy season, with average shifts of around 5 to 10 days for the Sahel (Dunning, 2018; IPCC, 2014; Pascale et al., 2016). Total precipitation is expected to decrease in the western parts and to increase in the central and eastern parts of the Sahel, although a high variability remains among the different climate model predictions (Biasutti, 2019; Pascale et al., 2016). Furthermore, an increase in rain event intensity, coupled with a decrease in frequency has been observed in recent years (Panthou et al., 2014; Taylor et al., 2017) and is projected for the coming century (Dunning, 2018). Even though the region has a long history of adapting to drastic changes in rainfall (Mortimore, 2010), it is still uncertain how current and future changes in rainfall regimes will impact the plant functional responses in the Sahel and in drylands in general.

Dryland vegetation is known to respond in contrasting ways to intra-annual rainfall variability. An increased frequency of heavy rainfall events is reported to facilitate woody encroachment in savannah ecosystems (Kulmatiski and Beard, 2013; Zhang et al., 2019), but this response is modulated by the underlying soil texture, as a more intense rainfall leads to a lower tree cover on soils with a finer texture (Case and Staver, 2018). Other studies found that regions with a given amount of total seasonal rainfall have a higher woody cover under a more frequent but less intense rainfall climatology, which can be explained by differentiated tree and grass water use strategies (Good and Caylor, 2011; Xu et al., 2015, 2018). D'Onofrio et al. (2019) found a positive relationship between grass cover and rain event frequency, but only a weak link between tree cover and rainfall seasonality characteristics for arid regions (mean annual precipitation (MAP) $\leqq$ 630 mm). Zhang et al. (2018) found vegetation in semi-arid zones (300-700 mm) to be impacted significantly by the number of rainy days and timing of the wet season. A vegetation model study by Guan et al. (2018) did not find a significant difference in impacts between the different seasonal rainfall characteristics mentioned above, although less arid regions (MAP > 700 mm) depicted a stronger increase in gross primary productivity (GPP) with enhanced length of the season than with enhanced rain event intensity or frequency.

In order to gain a more detailed process-based insight in how dryland vegetation is affected by the distribution of rainfall over the rainy season, we used a dynamic vegetation model to study the impact and legacy of single anomalous rainy seasons on the vegetation. The approach presented here is therefore complementary to earlier studies, such as Guan et al. (2018), which mainly assessed the impact on the vegetation of long-term changes in intra-seasonal rainfall variability, informing on

https://doi.org/10.5194/bg-2020-175
Preprint. Discussion started: 2 July 2020

the ecosystem state under prolonged changes in rainfall regime. Hence, the vegetation response in such studies is subject to cumulative effects of repeated rainfall disturbances, obscuring the underlying mechanisms that drive these responses.

We aimed at assessing the impact of different rainfall scenarios on the vegetation response at four flux tower sites across the Sahel (Tagesson et al., 2016; Table 1), investigating the response of individual plant functional types (PFTs), and of the ecosystem as a whole. We parameterized the LPJ-GUESS dynamic global vegetation model (Smith et al., 2014) for the Dahra site in Senegal (Tagesson et al., 2015), using field measurements and a literature study. The model was evaluated at all sites by testing whether it significantly improved the representation of the site ecosystem fluxes and vegetation composition, relative to the published version of the model (Smith et al., 2014). The model experiments were set up as a disturbance event, where we altered the rainfall during one year in the meteorological driver time series. We changed the total rainfall together with one of the underlying seasonal characteristics (i.e. intensity, frequency or length), while keeping the other two characteristics invariant.

Adopting this approach, we addressed the following research questions: (1) how do years of extreme rainfall with different seasonal characteristics impact the fluxes and composition of dryland ecosystems in the Sahel in the period following the extreme event, and (2) how do the magnitude and legacy of these impacts vary across the different plant functional types?

Table 1. Overview of the different flux tower sites used in this study, together with the 1979-2016 mean annual precipitation and its standard deviation (MAP, mm year^{-1}) from the MSWEP v1.2 dataset (Beck et al., 2017) mean annual temperature (MAT, °C) from the WFDEI dataset (Weedon et al., 2014), FAO soil classification (FAO, 1988), and ecosystem type (Tagesson et al., 2016).

Site	Coordinates	MAP ± σ	MAT	Soil classification	Ecosystem type
Dahra, Senegal	15.40°N 15.43°W	339 ± 107	28.7	Luvic Arenosol	Shrubland savanna (3% tree cover)
Agoufou, Mali	15.34°N 1.48°W	258 ± 83.4	30.2	Ferralic Arenosol	Open woody savanna (4% tree cover)
Wankama, Niger	13.65°N 2.63°E	303 ± 67.8	29.5	Ferralic Arenosol	Fallow bush
Demokeya, Sudan	13.28°N 30.48°E	164 ± 65.1	28.1	Cambic Arenosol	Sparse acacia savanna (7% tree cover)

2 Methods

2.1 Study area

The Sahel is a semi-arid ecoclimatic transition zone, bridging the Sahara desert in the north with the Sudanian savanna in the south. It is usually defined by the 150 mm and 700 mm isohyets delineating its northern and southern borders, respectively. In this study we used data from four flux tower sites that have been established in the Sahel, measuring land-atmosphere carbon, water and energy exchanges, together with meteorological data (Tagesson et al., 2016; Table 1). The flux towers are

https://doi.org/10.5194/bg-2020-175
Preprint. Discussion started: 2 July 2020


Biogeosciences Discussions

located at Dahra in Senegal (DAH), Agoufou in Mali (AGG), Wankama Fallow in Niger (WFF), and Demokeya in Sudan (DEM). For a more detailed description of these sites, we refer to Tagesson et al. (2016) and the references therein.

2.2 Vegetation model

We used the LPJ-GUESS process-based dynamic global vegetation model, which simulates the global vegetation structure with its associated carbon, nitrogen and water cycles (Smith et al., 2014). Similar to many global models, LPJ-GUESS uses plant functional types to represent physiological, morphological and phenological differences in vegetation. Out of the 12 standard PFTs in LPJ-GUESS, three are relevant for the Sahel: tropical broadleaved evergreen trees, tropical broadleaved deciduous trees, and C4 grasses. Within each gridcell, LPJ-GUESS simulates plant growth based on competition for light, space, water and soil nitrogen between individuals from different PFTs. Processes related to photosynthesis, soil hydrology, respiration, stomatal conductance and phenology are simulated on a daily time step, while carbon allocation, establishment, mortality and wildfire disturbance (Thonicke et al., 2001) are accounted for at the end of each simulated year. To account for the heterogeneity in age distribution of ecosystems, for each run 100 replicate patches were forced with the same meteorological data but exposed to stochastic differences in disturbances.

Soil hydrology is represented by a two-layer bucket model with percolation between the layers and drainage at the bottom (Gerten et al., 2004). The upper layer has a depth of 0.5 m, while the lower layer is 1 m deep, adding up to a total soil depth of 1.5 m. Rainfall will replenish plant-available water in the upper layer up to field capacity, above which excess water will be expelled as surface runoff. The lower soil layer is supplied with water by percolation from the upper layer. Transpiration by plant canopies will in turn reduce the water content in both soil layers. Different PFTs can have different root biomass distributions across the soil layers, e.g. grasses will have 90% of their root biomass in the upper layer, while trees have deeper roots (Table 2). LPJ-GUESS has previously been used in Sub-Saharan Africa and other savanna studies as well, yet the parameterization of the PFTs has never been optimized for the drylands in the Sahel specifically (Baudena et al., 2015; Boke-Olén et al., 2018; Brandt et al., 2018; Lehsten et al., 2016).

Table 2. Important PFT parameter values used in LPJ-GUESS: photosynthetic pathway, specific leaf area (SLA, m^2 kgC^{-1}), wood density (WD, kgC m^{-3}), maximum daily evapotranspiration rate (emax, mm day^{-1}) and root distribution (RD, fraction of the root biomass in the upper and lower soil layer, respectively) (Gerten et al., 2004; Nielsen, 2016; Sibret, 2017).

PFT	Photo	SLA	WD	emax	RD
C_4 grass	C_4	35.3	-	7	0.9 : 0.1
Evergreen Trees	C_3	13.9	319.1	5	0.6 : 0.4
Deciduous Trees	C_3	25.7	318.7	5	0.6 : 0.4

https://doi.org/10.5194/bg-2020-175
Preprint. Discussion started: 2 July 2020

2.3 Model parameterization and validation

We adjusted the parameterization of LPJ-GUESS to the local conditions by updating two plant functional traits (specific leaf area and wood density) to values from Nielsen (2016) and Sibret (2017). The tropical evergreen tree PFT was based on Balanites aegyptiaca, while the deciduous tree PFT was based on Acacia tortilis and Acacia senegal, which are the main woody species found at Dahra, Senegal. For the C4 grass parameters we used the average trait values of all C4 grasses identified by Sibret (2017), and the maximum daily evapotranspiration rate from Gerten et al. (2004). The most important parameters to differentiate the PFTs are given in Table 2. Similar species, or at least a functionally similar vegetation composition, can be found at the other three sites. All sites were assumed to have the same sandy soil texture in the simulations (90% sand, 5% silt, 5% clay).

The model was evaluated against flux tower data from the four Sahel sites by comparing a 10-day moving average of the measured daily net ecosystem productivity (NEP) and evapotranspiration (ET) time series with model predictions. Model performance metrics were summarized in a Taylor diagram (Taylor, 2001).

2.4 Model forcing timeline

By default, LPJ-GUESS is driven by daily interpolations of monthly Climatic Research Unit and National Centers for Environmental Prediction (CRU-NCEP) meteorological forcing data (Viovy, 2018). To improve the temporal resolution of the meteorological forcing, we used meteorological data extracted from WATCH Forcing Data methodology applied to ERA-Interim reanalysis (WFDEI; Weedon et al., 2014) with substituted Multi Source Weighted Ensemble Precipitation v1.2 data (MSWEP; Beck et al., 2017, 2019) instead. Both reanalysis datasets contain daily averages of meteorological data from 1979 to 2016 (Fig. 1). The data have a 0.5° by 0.5° spatial resolution and only the grid cells containing the flux tower locations were selected. Vegetation demography and its associated carbon, water and nitrogen stocks were initialized in the model by a 500-year spin-up run from bare soil. During this spin-up run the meteorological forcing data were used in a cycle, combined with a constant CO2 concentration of 296 ppm, corresponding to the 1901 level. The spin-up run was followed by a historical run from 1901 until 2016, using the same cycled meteorological forcing, but following the historical CO2 record. After this historical run, the rainfall perturbation experiments were implemented. In order to account for variability in meteorological conditions prior to the perturbation, the perturbations took place during the last year of a variable period of 1 to 37 years (one cycle of the meteorological drivers) past 2016. For this period, a constant CO2 concentration (the 2016 value of 404 ppm) was applied (Fig. 2).

https://doi.org/10.5194/bg-2020-175
Preprint. Discussion started: 2 July 2020

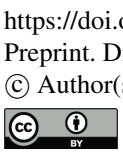

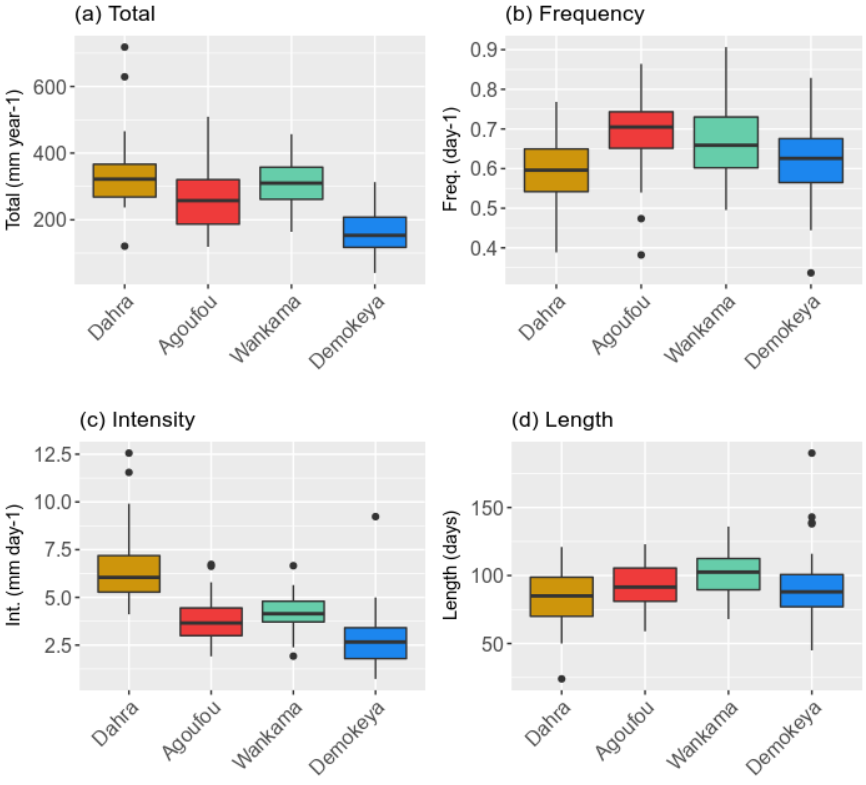

160 **Figure 1.** Median and variability of the rainy season characteristics for the Sahel sites (Table 1) studied: (a) total annual rainfall, (b) event frequency, (c) event intensity and (d) rainy season length. Hinges represent the first and third quartiles, whiskers represent the largest (smallest) value at most 1.5 times the interquartile range above (below) the hinges, and dots represent outliers. Based on the daily MSWEP rainfall data for the period 1979-2016.

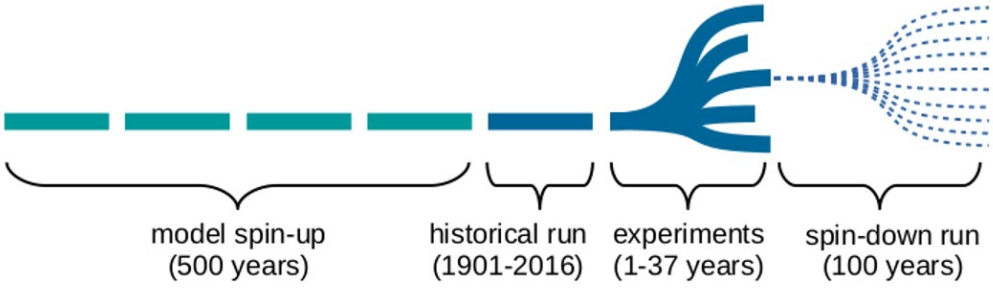

165 **Figure 2.** Overview of the general simulation timeline for each scenario. During the experiment period, one single year of the meteorological time series is disturbed, as illustrated by the different branches, and immediately followed by an

https://doi.org/10.5194/bg-2020-175
Preprint. Discussion started: 2 July 2020

ensemble of spin-down runs, consisting of average rainfall years only. Each horizontal segment represents a cycle of meteorological forcing data.

2.5 Disturbance experiment set-up

The rainfall disturbance experiments were developed to depict an increase or decrease of the total precipitation in a given year by two standard-deviations of the annual rainfall, therefore representative of extreme years in the historical time series. This disturbance was applied in such a way that only one of the three seasonal characteristics (intensity, frequency or length; Table 3) changed, while the other two remained invariant, thus creating a target rainy season for the selected year (Table 4). A detailed description of the used algorithms can be found in Supplementary Materials S1. In order to preserve the internal meteorological consistency with the other drivers (air temperature and incoming short-wave radiation), we resampled all data from the original meteorological drivers: for each DOY in the goal scenario, we found a date with matching rainfall (±1 mm) in the original dataset and used all its meteorological data. Some restrictions were introduced in order to preserve general synoptic patterns: the resampled day should be close to the original DOY (±3 days, ±1 year) and if none were found, the neighbouring pixels from the reanalysis dataset were consulted. If still no day with matching rainfall was found, the time interval was gradually extended in days until a match was found, up to a maximum of ±40 days.

Table 3. Definitions of the different rainy season characteristics used in this study.

Characteristic	Definition
Total rain	Total rainfall within the rainy season (mm).
Season start	Day of year after the minimum in climatological anomalous accumulation. Similar definition for the season end (DOY).
Season length	Difference between season start and end day of the year (days).
Intensity	Average daily total rainfall over all rainy days within the rainy season (mm day^{-1}).
Frequency	Inverse of average time (days) between rain events within the rainy season (day^{-1}).

The six simulation scenarios (Table 4) were applied to each year of the meteorological cycle that had a total rainfall close (±1σ) to the time series average, in order to avoid applying additional perturbations to already extreme years. Depending on the variability in annual rainfall for each site, this results in Ne≈30 simulations (Fig. 2). Each disturbed year was immediately followed by a set (Ns=10) of spin-down runs, each run consisting of a random 100-year sequence with rainfall within one standard deviation of the time series average. This was implemented to average out any effects of the post-disturbance years' rainfall characteristics on our impact study. For this 100-year sequence, the same constant CO2 concentration (the 2016 value of 404 ppm) was applied.

https://doi.org/10.5194/bg-2020-175
Preprint. Discussion started: 2 July 2020

Table 4. Overview of the scenarios with actual rainy season characteristic values for the Dahra site (average and standard deviation taken over all ensemble members).

Scenario	Rainfall disturbance	Modified characteristic
Len+	+186 ± 25.6 mm	+73.3 ± 18.3 days
Freq+	+203 ± 26.6 mm	+0.365 ± 0.079 events/day
Int+	+177 ± 57.9 mm	+3.321 ± 1.737 mm/event
Len-	-206 ± 11.8 mm	-62.5 ± 21.8 days
Freq-	-209 ± 11.8 mm	-0.426 ± 0.077 events/day
Int-	-209 ± 10.3 mm	-4.179 ± 0.974 mm/event

For each of these disturbance runs, a reference run was included, based on exactly the same meteorological data but without applying the perturbation in the disturbance year. This leads to an internally consistent set of meteorological model drivers for all six disturbance scenarios (Table 4), each simulated by an ensemble of Ne×Ns≈300 runs at four Sahel sites (Fig. 2). For each site and each scenario, the vegetation response was finally quantified as the difference between the output of the reference and disturbance runs, displayed as a function of time since the disturbance event and finally averaged over all ensemble members. We analyzed the response of individual PFTs, as well as the ecosystem as a whole, by quantifying the impact on leaf area index (LAI) and carbon cycling.

3 Results

3.1 Model evaluation

The updated parameterization of LPJ-GUESS captures the net ecosystem productivity (NEP) and evapotranspiration (ET) that were measured at the Dahra flux tower site (Fig. 3). Carbon uptake follows the timing of the rainy season, but the amplitude of both NEP and ET are underestimated over the whole time series. However, the fluxes measured at the Dahra site are relatively high when compared to the other Sahel sites (Tagesson et al., 2016). When evaluated against daily NEP measurements of the other Sahel sites, this parameterization significantly improves the agreement between simulated and observed daily carbon fluxes with respect to the published model parameterization, also when the latter is driven by the WFDEI-MSWEP meteorological forcing data which are used in this study (Fig. 4; Fig. S1). Interestingly, the improvement with respect to the published parameterization is larger for the other Sahel sites than for the Dahra site. In addition, we note that yearly averaged simulated values of surface runoff vary between sites from 16 mm/year to 49.8 mm/year, although the runoff distributions have a long tail due to extreme years. Indeed, median runoff values are much lower, varying between 4.4 mm/year and 30 mm/year (Fig. S2).

https://doi.org/10.5194/bg-2020-175
Preprint. Discussion started: 2 July 2020

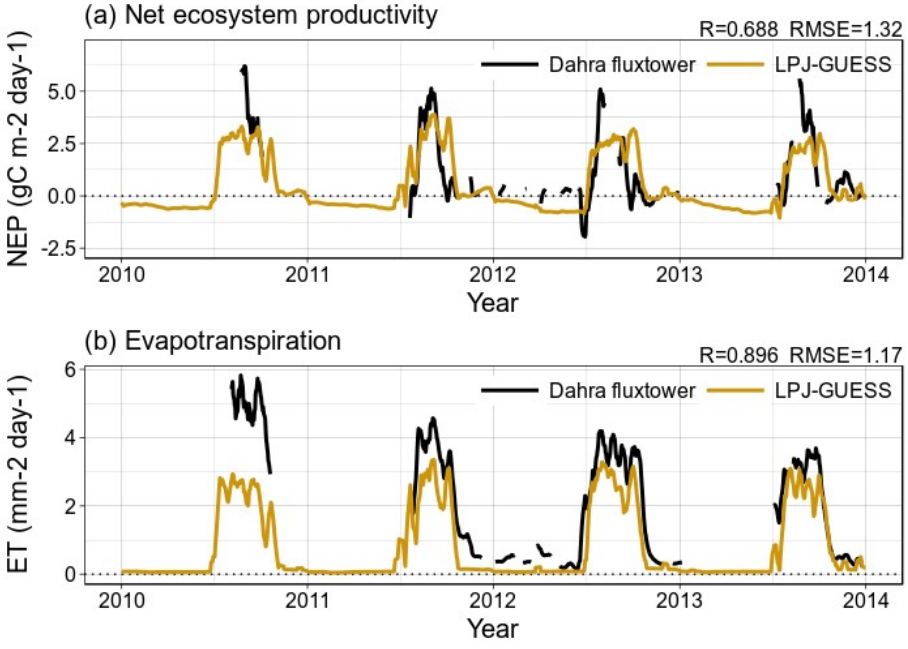

Figure 3. Time series of a 10-day moving average of (a) daily net ecosystem productivity (NEP) and (b) daily evapotranspiration (ET), comparing measurements from the flux tower near Dahra, Senegal with model results from LPJ-GUESS, using the Sahel-specific parameterization and WFDEI-MSWEP meteorological drivers.

https://doi.org/10.5194/bg-2020-175
Preprint. Discussion started: 2 July 2020

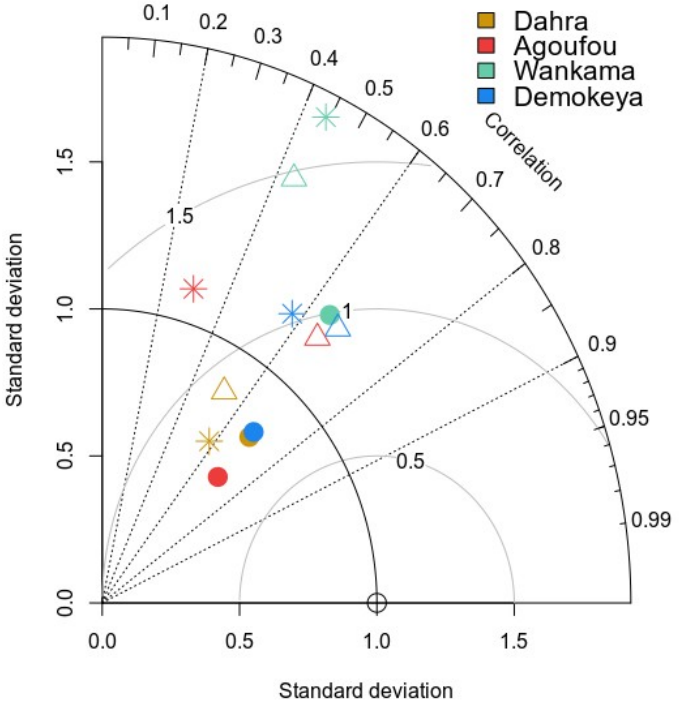

Figure 4. Taylor diagram showing the correspondence between modelled and observed daily NEP values (10-day moving averages) for the Sahel flux tower sites. We show a comparison between runs based on published model parameters using CRU-NCEP meteorological data (✳), published model version parameters using WFDEI-MSWEP drivers (△), and runs based on the new drylands-specific parameterization using the WFDEI-MSWEP drivers (●). Values were normalized so that the standard deviations of the observations equal unity, i.e. observations are located at the (1,0) coordinate on this figure Grey arcs represent the root mean square difference (RMSD) between model output and observations.

3.2 Experiment results

The impact of the different scenarios on vegetation abundance (Table 4) at the Dahra site was most significant for the C4 grasses, which showed a larger relative change in leaf area index (LAI) in response to the scenario's disturbances than the evergreen or deciduous trees (Fig. 5). Among the woody PFTs, the deciduous trees were impacted the least for all scenarios. An increased rainy season length generally induced a stronger response than scenarios of increased rain event frequency or intensity, especially for the LAI of C4 grasses (+122%) and evergreen trees (+54%). In contrast, for the scenarios of decreased total rainfall, the reduction was largely independent of the rainy season characteristic that was adjusted, although scenarios of decreased rainfall intensity depicted a slightly lower decline in LAI (Fig. 5).

Grasses respond immediately to changes in precipitation, with the highest impact occurring during the perturbed year (Fig. 5d). The responses to positive disturbances decay after ~4 years, while negative disturbances have a longer lasting impact (~6 years). Contrary to the herbaceous vegetation, both woody PFTs exhibited their peak impact in the year following the

https://doi.org/10.5194/bg-2020-175
Preprint. Discussion started: 2 July 2020

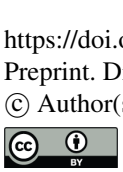

Biogeosciences Discussions Open Access EGU

disturbance and the legacy of the impact lasted considerably longer (up to 10-20 years) (Fig. 5e,f). Similar to grasses, positive impacts decay during a shorter timeframe than negative impacts for both woody PFTs. Although positive rainfall disturbances initially increase the LAI of both woody PFTs, evergreen trees benefit from this disturbance longer than deciduous trees, which are negatively impacted after the initial positive impact. This reversal in response is the most pronounced for the scenario of increased rainy season length, where the initial +22% increase in LAI is followed by a decrease to -17% in the sixth year after the disturbance event, possibly due to increased competition for soil water with the other PFTs (Fig. 5f). The opposite behaviour occurs for scenarios of decreased rainfall, in which the initial decrease in deciduous tree LAI (-40%) is followed by a positive impact up to +7% of the reference value. Depending on the scenario, these (positive or negative) overshoots last from 5 up to 20 years. For evergreen trees the overshoots are less pronounced and lower in magnitude than the model variability (Fig. 5e).

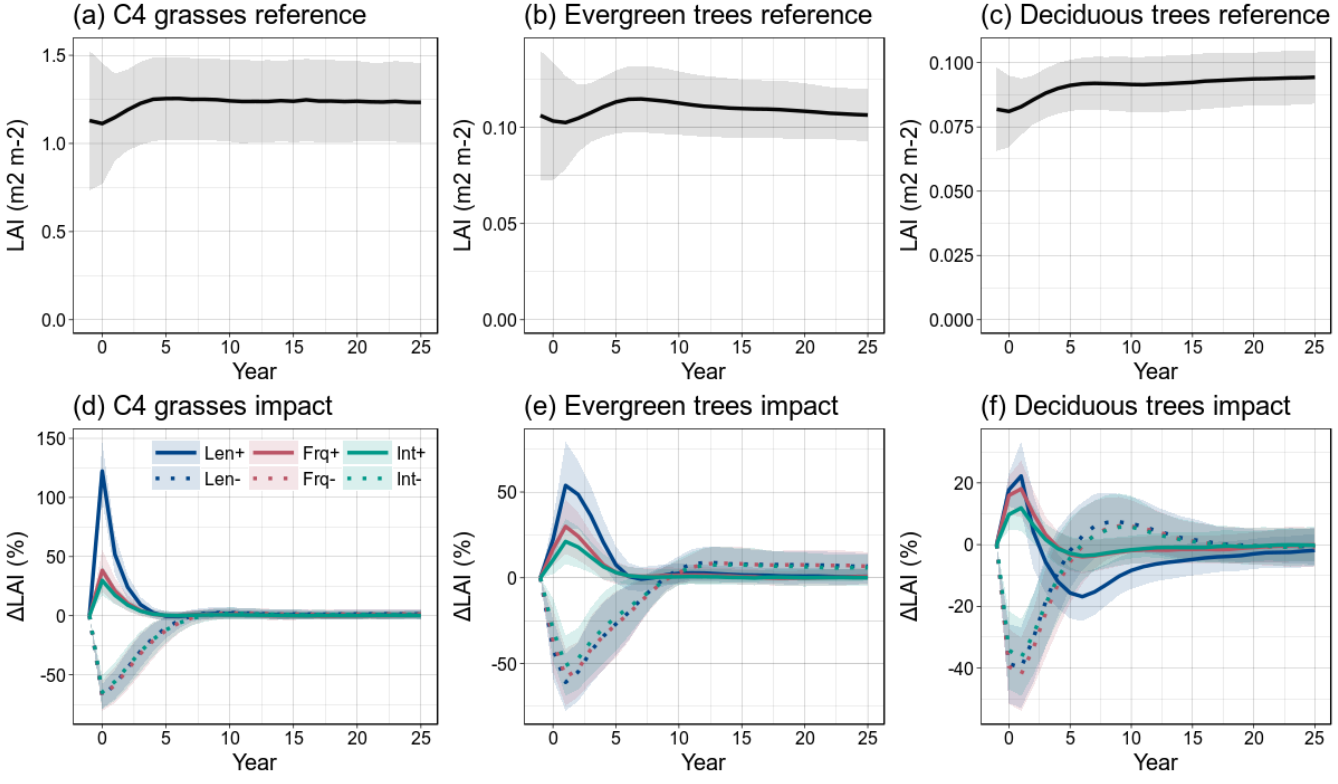

Figure 5. Response of the vegetation to the different rainfall scenarios for the Dahra site, in function of years since the disturbance event. (a-c) reference LAI of each PFT, averaged over all ensemble members; (d-f) vegetation response as the mean relative LAI difference between the scenario runs and the reference runs. Shaded areas indicate variability of the model runs over all ensemble members (±1σ).

https://doi.org/10.5194/bg-2020-175
Preprint. Discussion started: 2 July 2020

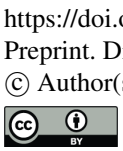

In order to study the long-term integrated response of each PFT, we calculated the difference in cumulative net primary productivity (NPP) between the disturbance and reference runs (Fig. 6). In the long run, grasses photosynthesize an additional 0.116 kgC m-2 for the scenarios of increased frequency or intensity, which corresponds to 0.53 times the average yearly uptake of the grasses in the reference run. For the long rainy season scenario, this increases up to 0.349 kgC m-2 (1.60 times the typical yearly reference NPP). For scenarios of decreased precipitation, the carbon uptake decreases by 0.436 kgC m-2 (~2 times avg. ref. NPP; Fig. 6a,d). Interestingly, evergreen trees perform relatively better than the grasses, compared to their respective reference uptake. Increased precipitation leads to an additional photosynthesis of 0.016 to 0.060 kgC m-2, which corresponds to 0.71 to 2.6 times the average reference NPP, while decreased precipitation will have a net uptake that is -0.012 to -0.0064 kgC m-2 below the reference value (-0.56 to -0.28 avg. ref. NPP; Fig. 6b,e). For deciduous trees, all scenarios lead to a total photosynthesis below the reference values, although the accumulated model variability becomes high towards the end of the studied period (Fig. 6c,f).

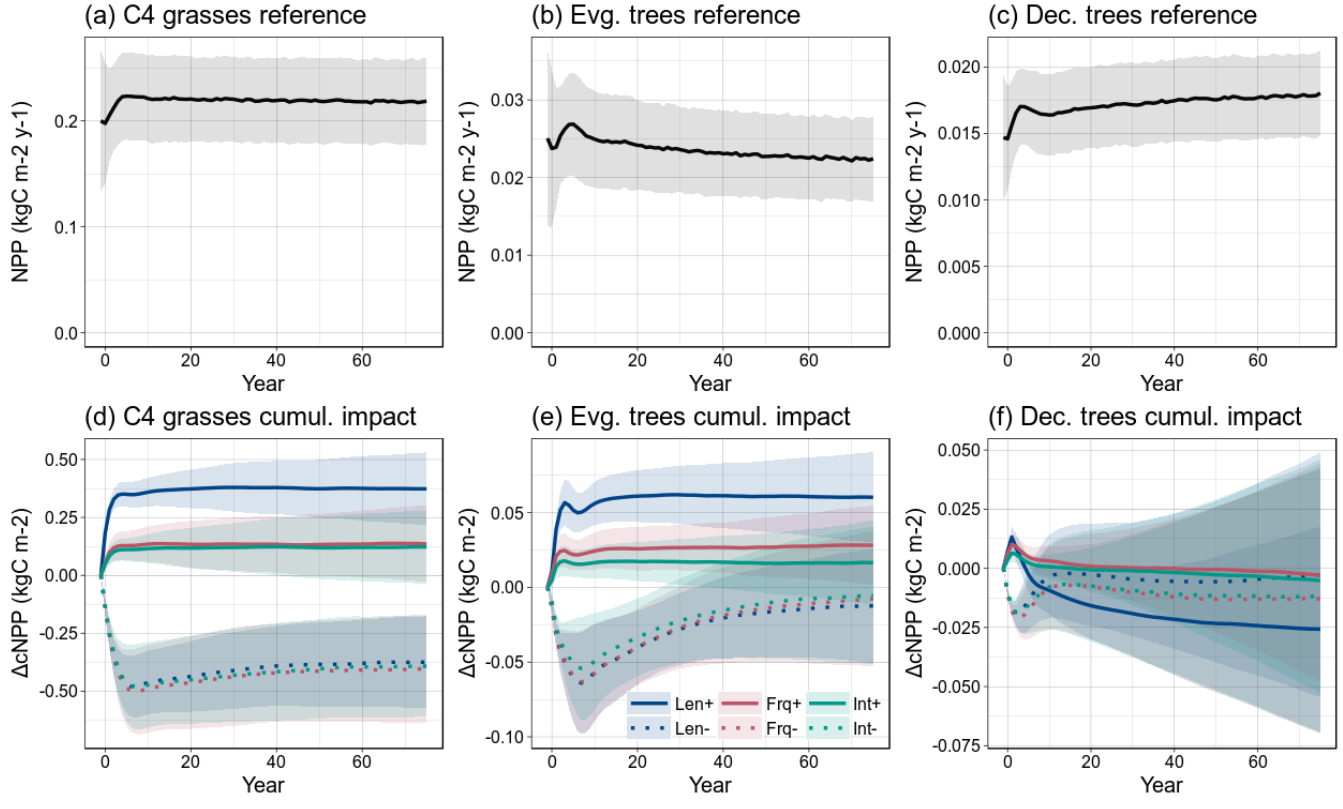

Figure 6. Impact on the cumulative net primary carbon uptake (NPP) for each PFT. (a-c) reference yearly NPP of each PFT; (d-f) difference in cumulative NPP with the reference run since the disturbance, divided by the average yearly NPP of the reference run. Expressed in units of years this gives how much years of typical production the PFT has lost or gained in the

https://doi.org/10.5194/bg-2020-175
Preprint. Discussion started: 2 July 2020

long run due to the perturbations. Shaded areas indicate variability of the model runs over all ensemble members (±1σ). Results shown for the Dahra site simulations.

When taking into account heterotrophic respiration processes by studying the net ecosystem productivity, the reference run simulated a NEP which was mostly positive and ranging between -8 and 19 gC m-2 year-1 (Fig. 7a). The cumulative yearly NEP of the reference run converged to a total uptake of 0.12 kgC m-2 over a 70-year period since the disturbance (Fig. 7c). Rainfall disturbance scenarios had a major impact on ecosystem productivity, with NEP values typically an order of magnitude above the reference. Increased rainfall scenarios amplified the carbon uptake with values ranging from 0.045 to 0.163 kgC m-2 year-1, while scenarios of decreased rainfall reduced NEP by values around -0.15 kgC m-2 year-1 (Fig. 7b). All disturbance scenarios displayed a substantial reversal in their NEP impact response, starting 2-3 years after the disturbance. The maximum amplitude of this reversal is 82% to 54% lower than the initial impact, but it takes several years to converge back to reference NEP values, its duration being asymmetrical between positive (6-7 years) and negative disturbances (11 years). The net effect of this reversal on the cumulative NEP is to balance out the initial impact on the long run, which can take several decades, depending on the scenario (Fig. 7d).

https://doi.org/10.5194/bg-2020-175
Preprint. Discussion started: 2 July 2020

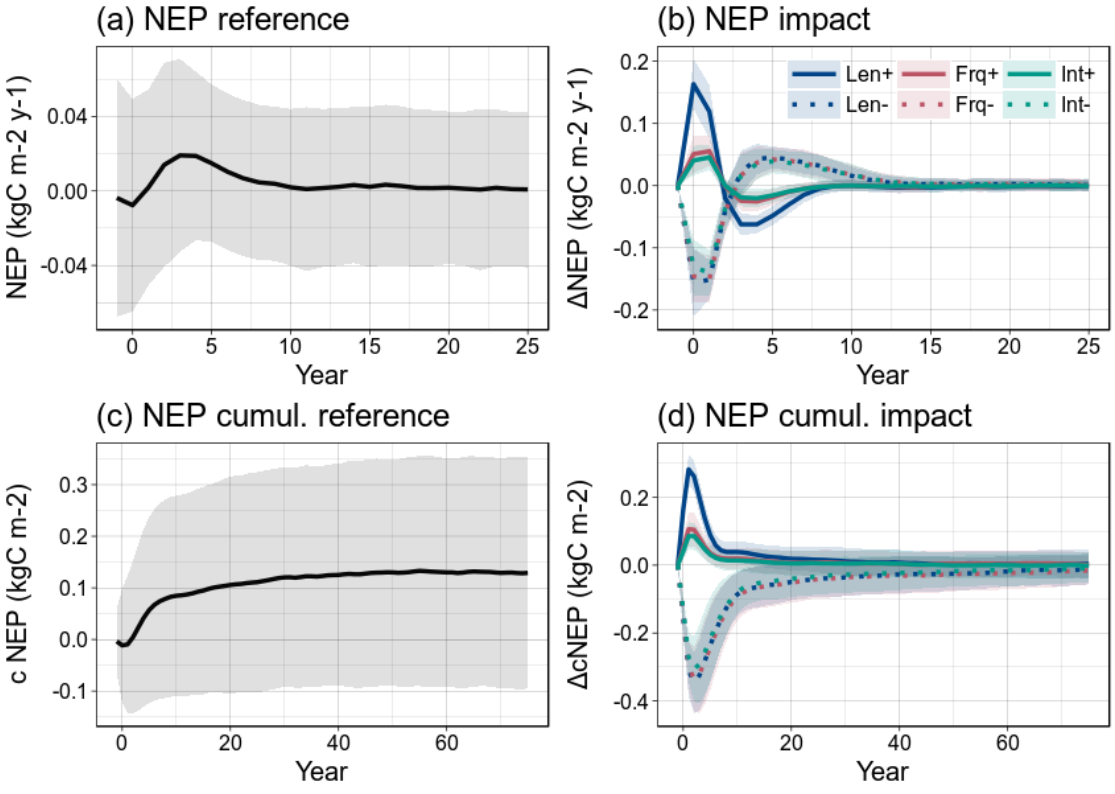

Figure 7. Impact of the different scenarios on the cumulative NEP. (a) Average reference yearly NEP over a period of 25 years after the disturbance. (b) Impact of the disturbances on yearly NEP. (c) Average reference cumulative NEP on a longer time scale (70 years). (d) Impact of the disturbances on the cumulative NEP. The year prior to the perturbations is used as a starting point for the cumulative sum. Shaded areas indicate variability of the model runs over all ensemble members (±1σ). Results shown for the Dahra site simulations.

The disturbance scenarios have a different impact on the surface balance between water evaporation, runoff and infiltration into the soil (Fig. 8). For disturbances that are based on a higher event frequency or a higher rainfall intensity, a quarter of the additional rainfall is immediately lost to surface evaporation (Fig. 8b) and around half is lost to runoff (Fig. 8d), so that the resulting amount of infiltrated water will be reduced accordingly (Fig. 8f). For the scenario with an increased rainy season length, there is only a slight increase in runoff because the rainfall has more time to percolate through the soil before saturation occurs. On the other hand, the scenarios with reduced precipitation all have similar impacts on surface water balance. During the years following the initial impact, the surface evaporation shows a significant reversal in response, with a magnitude of the same order as the initial impact. For the runoff this is only the case for the scenarios of decreased rainfall. All results shown in this section are for the Dahra site specifically, as this was the site for which the model was initially parameterized and validated. Qualitatively similar results were found for the other Sahel sites, although the relative

https://doi.org/10.5194/bg-2020-175
Preprint. Discussion started: 2 July 2020

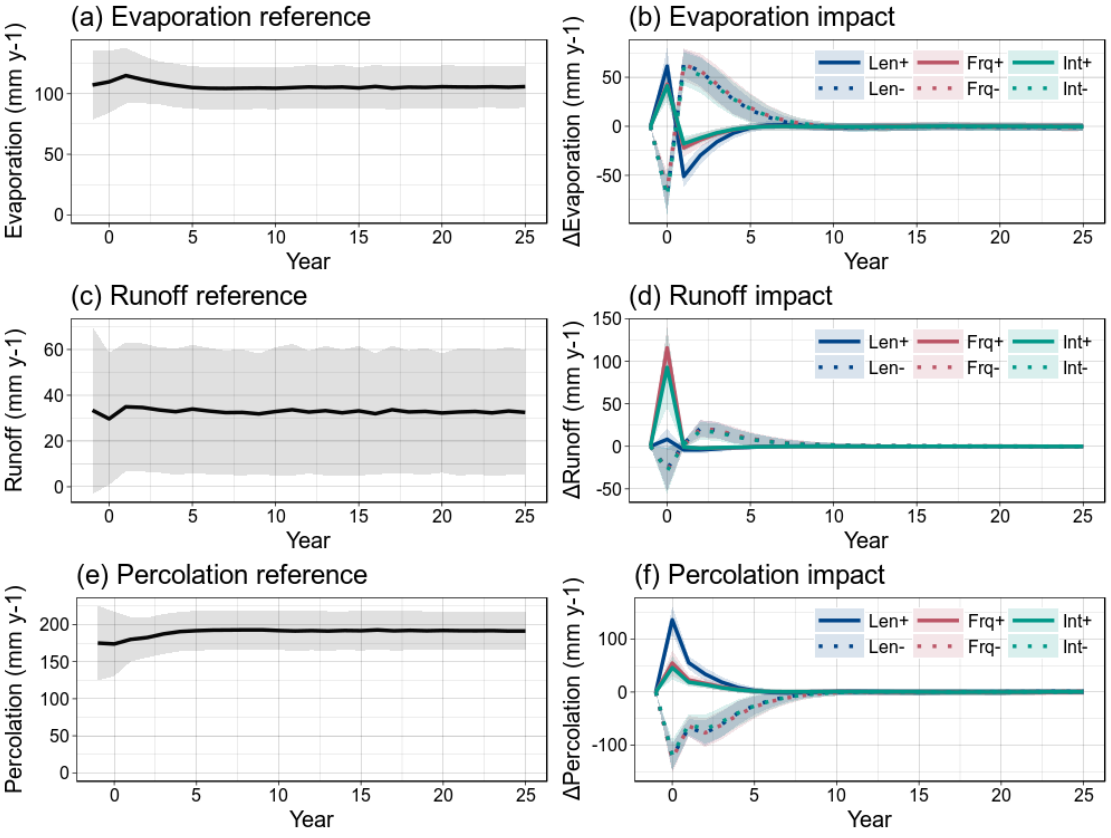

Figure 8. Impact of the different disturbance scenarios on surface water balance. Reference values and impact on (a,b) surface evaporation, (c,d) surface runoff, and (e,f) infiltration of water into the soil. Shaded areas indicate variability of the model runs over all ensemble members (±1σ). Results shown for the Dahra site simulations.

amplitudes and legacies of the scenarios varied due to differences in mean annual precipitation and its associated standard deviation, from which the amount of disturbance is calculated. Sites with a low MAP, such as Agoufou and Demokeya, generally show a longer legacy compared to the Dahra site, especially for negative disturbances (Supplementary Materials S3; Table 1).

Although fire can play a major role affecting the vegetation structure of African savannas, sites with a MAP below 350 mm are more rarely regulated by fire because of the low fuel availability (Sankaran et al., 2008). All sites considered in this study have a MAP of 339 mm or less (Table 1) and most fire events are anthropogenic. Nevertheless, as annual precipitation levels may increase under future climate scenarios, fires may play an increasing role at these sites in the future. The standard LPJ-GUESS model has a relatively simple fire module, where ignition is based on fuel load and litter moisture (Thonicke et al., 2001). In our study, fires only occurred at the wettest sites (Dahra and Wankama), when the fuel load was high and

https://doi.org/10.5194/bg-2020-175
Preprint. Discussion started: 2 July 2020

desiccated during a dry period following an occasional wet year. In these cases, fires mostly contributed for a small fraction (<3% of the GPP) to the total carbon flux, although there were a few exceptional years where the contribution was higher (6-11%). This was also observed in the disturbance experiments: for the rainfall exclusion scenarios, fires increased during the disturbed year due to reduced moisture, adding on average 1.8 to 40 gC m^{-2} $year^{-1}$ to the total carbon flux, depending on the scenario. For rainfall addition scenarios there was a peak in fires in the year after the disturbance due to increased litter, adding up to 10 gC m^{-2} $year^{-1}$ to the total carbon flux. However, for all scenarios the model uncertainty of the carbon fluxes due to fires was high, as the standard deviation of the impacts over all ensemble members was similar to the mean impact.

4 Discussion

4.1 Model evaluation

A combination of the updated model parameter values and daily scale WFDEI-MSWEP meteorological drivers improved the agreement between model simulations and flux tower measurements of NEP for all Sahel sites (Fig. 4). This is expected, as the published model PFTs (Smith et al., 2014) represent generic tropical species, while the new parameter values are specific for dryland ecosystems. A one-at-a-time sensitivity analysis revealed that updating other relevant parameters did not lead to a significant improvement in simulating the carbon fluxes and ET (not shown), but parameter covariance sensitivities are still to be tested. Moreover, the daily MSWEP data show a better match with precipitation measured at the flux tower (Fig. S3) and capture the onset and end of the rainy season better than the interpolated CRU-NCEP monthly data. Simulated reference values of surface runoff are relatively high when compared against earlier published ranges for the Sahel (Fekete et al., 2002). This has been observed in earlier land surface model intercomparison studies as well, stressing the need for a good representation of soil hydrology in vegetation models (Grippa et al., 2017).

4.2 Response of woody versus herbaceous cover

The herbaceous layer responded more strongly and swiftly to perturbations in precipitation than the woody vegetation for almost all sites and scenarios, especially to increases in rainy season length (Fig. 5). This contrasting behaviour reflects differences in plant representation in the model. Increased precipitation will lead to increased carbon uptake, which for grasses can be allocated to roots and leaves only. The tree PFTs will need to allocate a significant amount of carbon to woody components as well, which in turn will provide a safety net during the scenarios of decreased rainfall. The difference in the timing of the impact between grasses and trees is also partly due to the differences in root distribution. Grasses will be mostly affected by the water content in the upper soil layer, as it contains 90% of their root biomass in the model. Therefore, they will directly respond to changes in precipitation (Brandt et al., 2018; Gherardi and Sala, 2015). In contrast, trees have 40% of their root biomass in the lower soil layer of the model, where the water content integrates changes in precipitation over a longer timeframe. Together with physiological differences (e.g., allocation to woody parts), this explains the longer

https://doi.org/10.5194/bg-2020-175
Preprint. Discussion started: 2 July 2020

reaction time of the trees in the model. Further differences in response between evergreen and deciduous trees are due to their difference in SLA and phenology. Positive disturbances of increased rainfall initially benefit both woody PFTs, but the positive impacts last longer on evergreen trees, while the positive impacts on deciduous trees are followed by a negative overshoot, especially for the scenario of increased season length. Similarly, evergreen trees recover more slowly from negative disturbances than deciduous trees, which display a positive overshoot following the initial negative impact. These results show that single-year disturbances can shift the weights in the competition for resources among the different PFTs for several years. Kulmatiski and Beard (2013) have shown experimentally that an increase in rainfall intensity (without changing the total rainfall) will increase aboveground woody plant growth and decrease grass growth. This behaviour is not observed in our model study. However, as Kulmatiski and Beard (2013) argued, this increase reflects the ability of woody plants to increase their rooting depth, a process that is not included in our model, which only simulates two soil layers for which total root biomass can vary, but in which the PFT root distribution between the two layers remains fixed. Earlier research showed that the water use of Acacia tortillis trees in the Sahel is not much impacted by the dry season, as these trees have a deep taproot which reaches the water table (Do et al., 2008). Only after several dry years, when the water level in deeper soil layers plummets, this may have a major impact on tree water stress. A new model version of LPJ-GUESS is being developed, which will contain 15 soil layers and therefore may address these issues more adequately in the future.

On the ecosystem scale there is an increase in carbon uptake in response to a year of increased precipitation, but most of this gain is quickly lost again during the following years (Fig. 7). The largest part of the photosynthesised carbon will be allocated to leaf and root biomass of the C4 grasses, which will end up in the litter and soil carbon pools after the rainy season, where in turn most of it will respire again to the atmosphere during the following decades (Fig. S4). In response to a year of decreased precipitation, the ecosystem net productivity is reduced due to increased water stress on the plants, leading to a lower leaf production. During the years after this initial impact, the amount of leaf litter will therefore be lower than in the reference run. This causes a relative reduction in heterotrophic respiration and therefore a positive overshoot in the NEP impact. Nevertheless, it takes several decades before this increased NEP can balance out the initial carbon loss again (Fig. 7d). For all scenarios, the ecosystem proved to be resilient to single-year disturbances in precipitation, as no permanent change in ecosystem state was induced. However, the high magnitude and extensive legacy of the impacts of a single-year disturbance on ecosystem carbon uptake may potentially drive the high contribution of drylands to inter-annual variability in the global land carbon sink (Ahlstrom et al., 2015; Poulter et al., 2014).

Out of the three rainy season characteristics, a longer rainy season will have the highest impact on all PFTs and on the net ecosystem carbon uptake, which was corroborated for all four sites. This contrast between the scenarios was also simulated by Guan et al. (2018) for scenarios with long-term changes in precipitation, although only found for regions of higher mean annual precipitation (700-1600 mm year-1). Wu et al. (2018) reported a negative asymmetry in the response to exceptionally wet and dry years for temperate grasslands, where increases in aboveground net primary productivity (ANPP) were found to be smaller in magnitude during extremely wet years compared to decreases in ANPP during extreme dry years. The outcomes of our model experiments add a degree of nuance to these results, as we showed that the distribution of rainfall

https://doi.org/10.5194/bg-2020-175
Preprint. Discussion started: 2 July 2020

over the rainy season further modulates these asymmetrical responses: for the scenarios where rain event intensity or frequency were modified, the asymmetry was negative, while it was positive for scenarios in which season length was modified, i.e., increases in NPP due to a longer season had a larger magnitude than decreases due to a shorter season (Fig. S4). Wu et al. (2018) constructed their altered rainfall scenarios by increasing or decreasing the amount of rainfall in each event by a given factor, essentially producing scenarios of modified rainfall intensity (Supplementary Materials S1). The contrast between the scenarios is explained by the amount of water that infiltrates the soil (Fig. 8), as the same asymmetry in the distribution of water between scenarios with increased and decreased rainfall was found in the vegetation response. These results agree with earlier research showing that soil texture and structure may play a mediating role in the vegetation response to rainfall variability, although in our study only the sandy soil type was used (Case and Staver, 2018). These results may also clarify why models better capture the response of vegetation to rainfall exclusion than addition in the study of Paschalis et al. (2020), as the impact of scenarios of decreased rainfall is much less dependent on the rainy season characteristics than the impact of increased rainfall scenarios. Further vegetation model experiments could test the sensitivity of our results to different soil types, as we expect an even stronger contrast between the characteristics for finer structured soil. In general, local variations in hydraulic conductivity are known to have a major impact on the local-scale water balance in the Sahel, where soil surface crusting plays an important role (Leauthaud et al., 2017; Velluet et al., 2014).

It is expected that variations between the different sites are largely due to differences in historical meteorological conditions, as all other model parameters remained the same across sites. Sites with a lower MAP, such as Agoufou and Demokeya, will conceive a lower vegetation cover and therefore a lower reference net productivity. As reproduction and the growth of new biomass depends directly on NPP in the model, these drier sites are likely to take more time to recover from the applied disturbances.

Finally, our results seem to contrast earlier research which has shown that phenology of cropland and grassland in Sub-Saharan Africa is mainly driven by photoperiodicity, while in our model a longer rainy season will cause a longer growing season (Adole et al., 2019). Photoperiodicity is only implemented for crop PFTs in LPJ-GUESS, while for the natural vegetation PFTs that were used in this study, simulated phenology is driven by water availability, and therefore follows the rainy season. However, at the local scale the importance of photoperiod is diminished in the Sahel. While individuals of several species are photoperiodic, phenological plasticity is strong and a longer rainy season does seem to bring a longer growing season due to cohort and species succession.

4.3 Strengths and limitations

The approach developed in this study presents a unique way to investigate the impact of different rainy season characteristics on the vegetation in the Sahel. Our algorithm allows us to create artificial rainfall scenarios which strongly resemble the original rainfall data, while also retaining the internal consistency with other meteorological variables. By introducing one single year of anomalous rainfall in the time series, the impact on the ecosystem can be quantified in both magnitude and timing. The use of large ensembles of such disturbance scenarios has enabled us to gain a detailed insight into the processes

https://doi.org/10.5194/bg-2020-175
Preprint. Discussion started: 2 July 2020

that drive this vegetation response in arid and semi-arid regions. These techniques may be applicable in other regions and may be used to answer similar questions related to climate sensitivity of ecosystems. While earlier research often focuses on the impact of intra-annual rainfall distribution and variability on tree cover, this work also takes into account the impact on grasses in drylands. Changes in ecosystem composition, such as woody encroachment, would manifest themselves over decadal timescales. Such changes are rather driven by changes in rainfall regimes than singular anomalous years, and therefore we do not expect such shifts to happen here. Applying extreme precipitation repeatedly over a variable number of consecutive years will potentially lead to a tipping point, after which the ecosystem does not recover to its original state. However, this is beyond the scope of this research and the question remains how realistic or useful such a threshold would be. Experimental verification of the results predicted by this model should be feasible, but the results of earlier in situ experimental studies (e.g., Kulmatiski and Beard, 2013) are difficult to link with this study. Finally, this study does not take into account possible asymmetries in the distribution of rainfall over the rainy season, as rainfall increases in the core wet season are found to impact herbaceous foliar mass, while increases in the early or late parts of the rainy season impact mainly woody foliage production (Brandt et al., 2019).

As this is a modelling study, its outcome is as reliable as the model assumptions and parameterization, in addition to the quality of the meteorological drivers. The representation of drought stress and hydraulic dynamics through the soil-plant-atmosphere continuum is expected to play an important role to determine the impact of drought response of ecosystems, especially in drylands (Medlyn et al., 2016). However, like many vegetation models, LPJ-GUESS has a relatively simple representation of these processes, based on empirical relationships (Gerten et al., 2004; Smith et al., 2014). Recently, efforts have been made to improve these processes in the Ecosystem Demography (ED) model, by including a representation of the hydraulic pathway through the plant, connecting phenology with hydraulic status, and by parameterizing the hydraulic model based on plant hydraulic traits (Xu et al., 2016). Adapting these or similar ideas for LPJ-GUESS will most likely improve both the validation and the reliability of the results presented in this study. The quality of soil hydrology representation in the model may have an influence on the results of this study as well, given the importance of runoff and percolation for the vegetation impact. Furthermore, implementing a photoperiodicity-driven phenology may be necessary to upscale this research to the regional level (Adole et al., 2019). Finally, although fires play a major role in regulating woody cover in African savannas, its impact was limited for the (semi-)arid sites in this study and the model uncertainty was high where fires occurred. Most likely fire will play a larger role at lower latitudes, where the MAP levels are sufficient to generate the necessary fuel load for fires to occur. Studying the impact of rainfall disturbances on fire occurrence in those regions will lead to a better understanding of the complex disturbance-driven dynamics of mesic savannas (Sankaran et al., 2008), especially when LPJ-GUESS is coupled with more sophisticated fire models such as SPITFIRE, which significantly improve the fire model performance in those regions (Thonicke et al., 2010).

https://doi.org/10.5194/bg-2020-175
Preprint. Discussion started: 2 July 2020

Author contribution. W.V., G.S., S.H. and H.V. designed the research. W.V. performed model experiments and analysed the data. J.Ä., P.N.B, B.C., J.D., R.F., L.K. T.S. and T.T. collected the field data. W.V. drafted the paper and all authors contributed to writing the manuscript.

Competing interests. The authors declare that they have no conflict of interest.

Acknowledgements. The authors acknowledge the support for the U-TURN (Understanding Turning Points in Dryland Ecosystem Functioning, SR/00/339) project from the Belgian Federal Science Policy Office (BELSPO) in the framework of the STEREO III (Support to Exploitation and Research in Earth Observation) programme. Furthermore, the authors would like to sincerely thank Dr. M. Combe for the fruitful discussions, and M. Mbaye for the local support in Senegal.

References

Adole, T., Dash, J., Rodriguez-Galiano, V. and Atkinson, P. M.: Photoperiod controls vegetation phenology across Africa, Commun. Biol., 2(1), doi:10.1038/s42003-019-0636-7, 2019.

Ahlstrom, A., Raupach, M. R., Schurgers, G., Smith, B., Arneth, A., Jung, M., Reichstein, M., Canadell, J. G., Friedlingstein, P., Jain, A. K., Kato, E., Poulter, B., Sitch, S., Stocker, B. D., Viovy, N., Wang, Y. P., Wiltshire, A., Zaehle, S. and Zeng, N.: The dominant role of semi-arid ecosystems in the trend and variability of the land CO2 sink, Science (80-.)., 348(6237), 895–899, doi:10.1126/science.aaa1668, 2015.

Baudena, M., Dekker, S. C., Van Bodegom, P. M., Cuesta, B., Higgins, S. I., Lehsten, V., Reick, C. H., Rietkerk, M., Scheiter, S., Yin, Z., Zavala, M. A. and Brovkin, V.: Forests, savannas, and grasslands: Bridging the knowledge gap between ecology and Dynamic Global Vegetation Models, Biogeosciences, 12(6), 1833–1848, doi:10.5194/bg-12-1833-2015, 2015.

Beck, H. E., Vergopolan, N., Pan, M., Levizzani, V., van Dijk, A. I. J. M., Weedon, G. P., Brocca, L., Pappenberger, F., Huffman, G. J. and Wood, E. F.: Global-scale evaluation of 22 precipitation datasets using gauge observations and hydrological modeling, Hydrol. Earth Syst. Sci., 21(12), 6201–6217, doi:10.5194/hess-21-6201-2017, 2017.

Beck, H. E., Pan, M., Roy, T., Weedon, G. P., Pappenberger, F., Van Dijk, A. I. J. M., Huffman, G. J., Adler, R. F. and Wood, E. F.: Daily evaluation of 26 precipitation datasets using Stage-IV gauge-radar data for the CONUS, Hydrol. Earth Syst. Sci., 23(1), 207–224, doi:10.5194/hess-23-207-2019, 2019.

Berry, R. S. and Kulmatiski, A.: A savanna response to precipitation intensity, PLoS One, 12(4), 1–18, doi:10.1371/journal.pone.0175402, 2017.

Biasutti, M.: Rainfall trends in the African Sahel: Characteristics, processes, and causes, Wiley Interdiscip. Rev. Clim. Chang., 10(4), e591, doi:10.1002/wcc.591, 2019.

Boke-Olén, N., Lehsten, V., Abdi, A. M., Ardö, J. and Khatir, A. A.: Estimating Grazing Potentials in Sudan Using Daily Carbon Allocation in Dynamic Vegetation Model, Rangel. Ecol. Manag., 71(6), 792–797, doi:10.1016/j.rama.2018.06.006, 2018.

https://doi.org/10.5194/bg-2020-175
Preprint. Discussion started: 2 July 2020

Brandt, M., Wigneron, J. P., Chave, J., Tagesson, T., Penuelas, J., Ciais, P., Rasmussen, K., Tian, F., Mbow, C., Al-Yaari, A., Rodriguez-Fernandez, N., Schurgers, G., Zhang, W., Chang, J., Kerr, Y., Verger, A., Tucker, C., Mialon, A., Rasmussen, L. V., Fan, L. and Fensholt, R.: Satellite passive microwaves reveal recent climate-induced carbon losses in African drylands, Nat. Ecol. Evol., 2(5), 827–835, doi:10.1038/s41559-018-0530-6, 2018.

Brandt, M., Hiernaux, P., Rasmussen, K., Tucker, C. J., Wigneron, J. P., Diouf, A. A., Herrmann, S. M., Zhang, W., Kergoat, L., Mbow, C., Abel, C., Auda, Y. and Fensholt, R.: Changes in rainfall distribution promote woody foliage production in the Sahel, Commun. Biol., 2(1), 1–10, doi:10.1038/s42003-019-0383-9, 2019.

Case, M. F. and Staver, A. C.: Soil texture mediates tree responses to rainfall intensity in African savannas, New Phytol., 219(4), 1363–1372, doi:10.1111/nph.15254, 2018.

Do, F. C., Rocheteau, A., Diagne, A. L., Goudiaby, V., Granier, A. and Lhomme, J. P.: Stable annual pattern of water use by Acacia tortilis in Sahelian Africa, Tree Physiol., 28(1), 95–104, doi:10.1093/treephys/28.1.95, 2008.

Dodd, M. B., Lauenroth, W. K. and Welker, J. M.: Differential water resource use by herbaceous and woody plant life-forms in a shortgrass steppe community, Oecologia, 117(4), 504–512, doi:10.1007/s004420050686, 1998.

Dunning, C.: Characterising and Understanding Trends and Variability in African Rainfall Seasonality., 2018.

FAO: FAO/Unesco Soil Map of the World, World Soil Resour. Rep. 60, 1988.

Fekete, B. M., Vörösmarty, C. J. and Grabs, W.: High-resolution fields of global runoff combining observed river discharge and simulated water balances, Global Biogeochem. Cycles, 16(3), 15-1-15–10, doi:10.1029/1999gb001254, 2002.

Gerten, D., Schaphoff, S., Haberlandt, U., Lucht, W. and Sitch, S.: Terrestrial vegetation and water balance - Hydrological evaluation of a dynamic global vegetation model, J. Hydrol., 286(1–4), 249–270, doi:10.1016/j.jhydrol.2003.09.029, 2004.

Gherardi, L. A. and Sala, O. E.: Enhanced precipitation variability decreases grass- and increases shrub-productivity, Proc. Natl. Acad. Sci. U. S. A., 112(41), 12735–12740, doi:10.1073/pnas.1506433112, 2015.

Gilbert, N.: Science enters desert debate, Nature, 477(7364), 262–262, doi:10.1038/477262a, 2011.

Good, S. P. and Caylor, K. K.: Climatological determinants of woody cover in Africa, Proc. Natl. Acad. Sci., 108(12), 4902–4907, doi:10.1073/pnas.1013100108, 2011.

Grace, J., José, J. S., Meir, P., Miranda, H. S. and Montes, R. A.: Productivity and carbon fluxes of tropical savannas, J. Biogeogr., 33(3), 387–400, doi:10.1111/j.1365-2699.2005.01448.x, 2006.

Grippa, M., Kergoat, L., Boone, A., Peugeot, C., Demarty, J., Cappelaere, B., Gal, L., Hiernaux, P., Mougin, E., Ducharne, A., Dutra, E., Anderson, M., Hain, C., Ait-Mesbah, S., Polcher, J., Balsamo, G., Boussetta, S., Pappenberger, F., Favot, F., Guichard, F., Kaptue, A., Roujean, J. L., Chaffard, V., Cohard, J. M., Gascon, T., Galle, S., Hector, B., Lebel, T., Pellarin, T., Richard, A., Quantin, G., Chan, E., Verseghy, D., Magand, C., Getirana, A., Pierre, C., Gusev, Y., Nasonova, O., Harris, P., He, X., Yorozu, K., Kotsuki, S., Tanaka, K., Kim, H., Oki, T., Kumar, S., Lo, M. H., Mahanama, S., Maignan, F., Ottlé, C., Mamadou, O., Shmakin, A., Sokratov, V. and Turkov, D.: Modeling Surface runoff and water fluxes over contrasted soils in the pastoral sahel: Evaluation of the ALMIP2 land surface models over the Gourma Region in Mali, J. Hydrometeorol., 18(7), 1847–1866, doi:10.1175/JHM-D-16-0170.1, 2017.

https://doi.org/10.5194/bg-2020-175
Preprint. Discussion started: 2 July 2020

Guan, K., Good, S. P., Caylor, K. K., Medvigy, D., Pan, M., Wood, E. F., Sato, H., Biasutti, M., Chen, M., Ahlström, A. and Xu, X.: Simulated sensitivity of African terrestrial ecosystem photosynthesis to rainfall frequency, intensity, and rainy season length, Environ. Res. Lett., 13(2), doi:10.1088/1748-9326/aa9f30, 2018.

Haub, C. and Toshiko, K.: 2014 World Population Data Sheet, Washington, DC Popul. Ref. Bur., 2014.

Ibrahim, F. N.: Causes of the famine among the rural population of the Sahelian zone of the Sudan, GeoJournal, 17(1), doi:10.1007/BF00209083, 1988.

IPCC: Future Climate Changes, Risks and Impacts., 2014.

Kulmatiski, A. and Beard, K. H.: Woody plant encroachment facilitated by increased precipitation intensity, Nat. Clim. Chang., 3(9), 833–837, doi:10.1038/nclimate1904, 2013.

Leauthaud, C., Cappelaere, B., Demarty, J., Guichard, F., Velluet, C., Kergoat, L., Vischel, T., Grippa, M., Mouhaimouni, M., Bouzou Moussa, I., Mainassara, I. and Sultan, B.: A 60-year reconstructed high-resolution local meteorological data set in Central Sahel (1950–2009): evaluation, analysis and application to land surface modelling, Int. J. Climatol., 37(5), 2699–2718, doi:10.1002/joc.4874, 2017.

Lehmann, C. E. R., Anderson, T. M., Sankaran, M., Higgins, S. I., Archibald, S., Hoffmann, W. A., Hanan, N. P., Williams, R. J., Fensham, R. J., Felfili, J., Hutley, L. B., Ratnam, J., San Jose, J., Montes, R., Franklin, D., Russell-Smith, J., Ryan, C. M., Durigan, G., Hiernaux, P., Haidar, R., Bowman, D. M. J. S. and Bond, W. J.: Savanna Vegetation-Fire-Climate Relationships Differ Among Continents, Science (80-.)., 343(6170), 548–552, doi:10.1126/science.1247355, 2014.

Lehsten, V., Arneth, A., Spessa, A., Thonicke, K. and Moustakas, A.: The effect of fire on tree-grass coexistence in savannas: A simulation study, Int. J. Wildl. Fire, 25(2), 137–146, doi:10.1071/WF14205, 2016.

McMurtrie, R. and Wolf, L.: A Model of Competition between Trees and Grass for Radiation, Water and Nutrients, Ann. Bot., 52(4), 449–458, doi:10.1093/oxfordjournals.aob.a086600, 1983.

Medlyn, B. E., De Kauwe, M. G. and Duursma, R. A.: New developments in the effort to model ecosystems under water stress, New Phytol., 212(1), 5–7, doi:10.1111/nph.14082, 2016.

Mortimore, M.: Adapting to drought in the Sahel: Lessons for climate change, Wiley Interdiscip. Rev. Clim. Chang., 1(1), 134–143, doi:10.1002/wcc.25, 2010.

Nielsen, I. B.: Ground based evidence of woody cover trends and an examination of the potential of the Senegalese Sahel as a carbon sink, Copenhagen University., 2016.

Panthou, G., Vischel, T. and Lebel, T.: Recent trends in the regime of extreme rainfall in the Central Sahel, Int. J. Climatol., 34(15), 3998–4006, doi:10.1002/joc.3984, 2014.

Pascale, S., Lucarini, V., Feng, X., Porporato, A. and ul Hasson, S.: Projected changes of rainfall seasonality and dry spells in a high greenhouse gas emissions scenario, Clim. Dyn., 46(3–4), 1331–1350, doi:10.1007/s00382-015-2648-4, 2016.

Paschalis, A., Fatichi, S., Zscheischler, J., Ciais, P., Bahn, M., Boysen, L., Chang, J., De Kauwe, M., Estiarte, M., Goll, D., Hanson, P. J., Harper, A. B., Hou, E., Kigel, J., Knapp, A. K., Larsen, K. S., Li, W., Lienert, S., Luo, Y., Meir, P., Nabel, J. E. M. S., Ogaya, R., Parolari, A. J., Peng, C., Peñuelas, J., Pongratz, J., Rambal, S., Schmidt, I. K., Shi, H., Sternberg, M., Tian, H., Tschumi, E., Ukkola, A., Vicca, S., Viovy, N., Wang, Y. P., Wang, Z., Williams, K., Wu, D. and Zhu, Q.: Rainfall

manipulation experiments as simulated by terrestrial biosphere models: Where do we stand?, Glob. Chang. Biol., (July 2019), 1–20, doi:10.1111/gcb.15024, 2020.

Poulter, B., Frank, D., Ciais, P., Myneni, R. B., Andela, N., Bi, J., Broquet, G., Canadell, J. G., Chevallier, F., Liu, Y. Y., Running, S. W., Sitch, S. and Van Der Werf, G. R.: Contribution of semi-arid ecosystems to interannual variability of the global carbon cycle, Nature, 509(7502), 600–603, doi:10.1038/nature13376, 2014.

Sankaran, M., Hanan, N. P., Scholes, R. J., Ratnam, J., Augustine, D. J., Cade, B. S., Gignoux, J., Higgins, S. I., Le Roux, X., Ludwig, F., Ardo, J., Banyikwa, F., Bronn, A., Bucini, G., Caylor, K. K., Coughenour, M. B., Diouf, A., Ekaya, W., Feral, C. J., February, E. C., Frost, P. G. H., Hiernaux, P., Hrabar, H., Metzger, K. L., Prins, H. H. T., Ringrose, S., Sea, W., Tews, J., Worden, J. and Zambatis, N.: Determinants of woody cover in African savannas., Nature, 438(7069), 846–849, doi:10.1038/nature04070, 2005.

Sankaran, M., Ratnam, J. and Hanan, N.: Woody cover in African savannas: The role of resources, fire and herbivory, Glob. Ecol. Biogeogr., 17(2), 236–245, doi:10.1111/j.1466-8238.2007.00360.x, 2008.

Sibret, T.: The Sahelian drylands under pressure: studying the impact of environmental factors on vegetation in Dahra, Senegal, Ghent University., 2017.

Sillmann, J., Kharin, V. V., Zwiers, F. W., Zhang, X. and Bronaugh, D.: Climate extremes indices in the CMIP5 multimodel ensemble: Part 2. Future climate projections, J. Geophys. Res. Atmos., 118(6), 2473–2493, doi:10.1002/jgrd.50188, 2013.

Smith, B., Wärlind, D., Arneth, A., Hickler, T., Leadley, P., Siltberg, J. and Zaehle, S.: Implications of incorporating N cycling and N limitations on primary production in an individual-based dynamic vegetation model, Biogeosciences, 11(7), 2027–2054, doi:10.5194/bg-11-2027-2014, 2014.

Tagesson, T., Fensholt, R., Guiro, I., Rasmussen, M. O., Huber, S., Mbow, C., Garcia, M., Horion, S., Sandholt, I., Holm-Rasmussen, B., Göttsche, F. M., Ridler, M.-E., Olén, N., Lundegard Olsen, J., Ehammer, A., Madsen, M., Olesen, F. S. and Ardö, J.: Ecosystem properties of semiarid savanna grassland in West Africa and its relationship with environmental variability, Glob. Chang. Biol., 21(1), 250–264, doi:10.1111/gcb.12734, 2015.

Tagesson, T., Fensholt, R., Cappelaere, B., Mougin, E., Horion, S., Kergoat, L., Nieto, H., Mbow, C., Ehammer, A., Demarty, J. and Ardö, J.: Spatiotemporal variability in carbon exchange fluxes across the Sahel, Agric. For. Meteorol., 226–227, 108–118, doi:10.1016/j.agrformet.2016.05.013, 2016.

Taylor, C. M., Belusic, D., Guichard, F., Parker, D. J., Vischel, T., Bock, O., Harris, P. P., Janicot, S., Klein, C. and Panthou, G.: Frequency of extreme Sahelian storms tripled since 1982 in satellite observations, Nature, 544(7651), 475–478, doi:10.1038/nature22069, 2017.

Taylor, K. E.: Summarizing multiple aspects of model performance in a single diagram, J. Geophys. Res. Atmos., 106(D7), 7183–7192, doi:10.1029/2000JD900719, 2001.

Thonicke, K., Venevsky, S., Sitch, S. and Cramer, W.: The role of fire disturbance for global vegetation dynamics: Coupling fire into a dynamic global vegetation model, Glob. Ecol. Biogeogr., 10(6), 661–677, doi:10.1046/j.1466-822X.2001.00175.x, 2001.

Thonicke, K., Spessa, A., Prentice, I. C., Harrison, S. P., Dong, L. and Carmona-Moreno, C.: The influence of vegetation, fire spread and fire behaviour on biomass burning and trace gas emissions: Results from a process-based model, Biogeosciences, 7(6), 1991–2011, doi:10.5194/bg-7-1991-2010, 2010.

United Nations Office for the Coordination of Humanitarian Affairs: Sahel Regional Strategy Mid-Year Review 2013, 2013.

Velluet, C., Demarty, J., Cappelaere, B., Braud, I., Issoufou, H. B. A., Boulain, N., Ramier, D., Mainassara, I., Charvet, G., Boucher, M., Chazarin, J. P., Oï, M., Yahou, H., Maidaji, B., Arpin-Pont, F., Benarrosh, N., Mahamane, A., Nazoumou, Y., Favreau, G. and Seghieri, J.: Building a field- and model-based climatology of local water and energy cycles in the cultivated Sahel - Annual budgets and seasonality, Hydrol. Earth Syst. Sci., 18(12), 5001–5024, doi:10.5194/hess-18-5001-2014, 2014.

Viovy, N.: CRUNCEP Version 7 - Atmospheric Forcing Data for the Community Land Model, Res. Data Arch. Natl. Cent. Atmos. Res. Comput. Inf. Syst. Lab. [online] Available from: https://rda.ucar.edu/datasets/ds314.3/ (Accessed 29 November 2019), 2018.

Wang, L., D'Odorico, P., Evans, J. P., Eldridge, D. J., McCabe, M. F., Caylor, K. K. and King, E. G.: Dryland ecohydrology and climate change: critical issues and technical advances, Hydrol. Earth Syst. Sci., 16(8), 2585–2603, doi:10.5194/hess-16-2585-2012, 2012.

Weedon, G. P., Balsamo, G., Bellouin, N., Gomes, S., Best, M. J. and Viterbo, P.: The WFDEI meteorological forcing data set: WATCH Forcing Data methodology applied to ERA-Interim reanalysis data, Water Resour. Res., 50(9), 7505–7514, doi:10.1002/2014WR015638, 2014.

Whitley, R., Beringer, J., Hutley, L. B., Abramowitz, G., De Kauwe, M. G., Evans, B., Haverd, V., Li, L., Moore, C., Ryu, Y., Scheiter, S., Schymanski, S. J., Smith, B., Wang, Y.-P., Williams, M. and Yu, Q.: Challenges and opportunities in land surface modelling of savanna ecosystems, Biogeosciences, 14(20), 4711–4732, doi:10.5194/bg-14-4711-2017, 2017.

van Wijk, M. T. and Rodriguez-Iturbe, I.: Tree-grass competition in space and time: Insights from a simple cellular automata model based on ecohydrological dynamics, Water Resour. Res., 38(9), 18-1-18–15, doi:10.1029/2001wr000768, 2002.

Wu, D., Ciais, P., Viovy, N., Knapp, A. K., Wilcox, K., Bahn, M., Smith, M. D., Vicca, S., Fatichi, S., Zscheischler, J., He, Y., Li, X., Ito, A., Arneth, A., Harper, A., Ukkola, A., Paschalis, A., Poulter, B., Peng, C., Ricciuto, D., Reinthaler, D., Chen, G., Tian, H., Genet, H., Mao, J., Ingrisch, J., Nabel, J. E. S. M., Pongratz, J., Boysen, L. R., Kautz, M., Schmitt, M., Meir, P., Zhu, Q., Hasibeder, R., Sippel, S., Dangal, S. R. S., Sitch, S., Shi, X., Wang, Y., Luo, Y., Liu, Y. and Piao, S.: Asymmetric responses of primary productivity to altered precipitation simulated by ecosystem models across three long-term grassland sites, Biogeosciences, 15(11), 3421–3437, doi:10.5194/bg-15-3421-2018, 2018.

Xu, X., Medvigy, D. and Rodriguez-Iturbe, I.: Relation between rainfall intensity and savanna tree abundance explained by water use strategies, Proc. Natl. Acad. Sci., 112(42), 12992–12996, doi:10.1073/pnas.1517382112, 2015.

Xu, X., Medvigy, D., Powers, J. S., Becknell, J. M. and Guan, K.: Diversity in plant hydraulic traits explains seasonal and inter-annual variations of vegetation dynamics in seasonally dry tropical forests, New Phytol., 212(1), 80–95, doi:10.1111/nph.14009, 2016.

Xu, X., Medvigy, D., Trugman, A. T., Guan, K., Good, S. P. and Rodriguez-Iturbe, I.: Tree cover shows strong sensitivity to precipitation variability across the global tropics, Glob. Ecol. Biogeogr., 27(4), 450–460, doi:10.1111/geb.12707, 2018.

https://doi.org/10.5194/bg-2020-175
Preprint. Discussion started: 2 July 2020

615 Zhang, W., Brandt, M., Guichard, F., Tian, Q. and Fensholt, R.: Using long-term daily satellite based rainfall data (1983–2015) to analyze spatio-temporal changes in the sahelian rainfall regime, J. Hydrol., 550, 427–440, doi:10.1016/j.jhydrol.2017.05.033, 2017.

Zhang, W., Brandt, M., Tong, X., Tian, Q. and Fensholt, R.: Impacts of the seasonal distribution of rainfall on vegetation productivity across the Sahel, Biogeosciences, 15(1), 319–330, doi:10.5194/bg-15-319-2018, 2018.

620 Zhang, W., Brandt, M., Penuelas, J., Guichard, F., Tong, X., Tian, F. and Fensholt, R.: Ecosystem structural changes controlled by altered rainfall climatology in tropical savannas, Nat. Commun. 2019 101, 10(1), 671, doi:10.1038/s41467-019-08602-6, 2019.